Available online at www.sciencedirect.com

ScienceDirect

Advances in Space Research 47 (2011) 1006–1019

ADVANCES IN SPACE RESEARCH (a COSPAR publication)

www.elsevier.com/locate/asr

# On the effect of considering more realistic particle shape and mass parameters in MMOD risk assessments

Joel E. Williamsen [a], William P. Schonberg [b,*], Alan B. Jenkin [c]

[a] Institute for Defense Analyses, 4850 Mark Center Drive, Alexandria, VA, United States
[b] Civil, Architectural, and Environmental Engineering Department, Missouri University of Science and Technology, Rolla, MO 65409, United States
[c] The Aerospace Corporation, 2350 E El Segundo Blvd, El Segundo, CA 90245-4691, United States

Received 6 July 2010; received in revised form 6 November 2010; accepted 8 November 2010
Available online 13 November 2010

**Abstract**

One of the primary mission risks tracked in the development of all spacecraft is that due to micro-meteoroids and orbital debris (MMOD). Both types of particles, especially those larger than 0.1 mm in diameter, contain sufficient kinetic energy due to their combined mass and velocities to cause serious damage to crew members and spacecraft. The process used to assess MMOD risk consists of three elements: environment, damage prediction, and damage tolerance. Orbital debris risk assessments for the Orion vehicle, as well as the Shuttle, Space Station and other satellites use ballistic limit equations (BLEs) that have been developed using high speed impact test data and results from numerical simulations that have used spherical projectiles. However, spheres are not expected to be a common shape for orbital debris; rather, orbital debris fragments might be better represented by other regular or irregular solids. In this paper we examine the general construction of NASA's current orbital debris (OD) model, explore the potential variations in orbital debris mass and shape that are possible when using particle characteristic length to define particle size (instead of assuming spherical particles), and, considering specifically the Orion vehicle, perform an orbital debris risk sensitivity study taking into account variations in particle mass and shape as noted above. While the results of the work performed for this study are preliminary, they do show that continuing to use aluminum spheres in spacecraft risk assessments could result in an *over*-design of its MMOD protection systems. In such a case, the spacecraft could be heavier than needed, could cost more than needed, and could cost more to put into orbit than needed. The results obtained in this study also show the need to incorporate effects of mass and shape in mission risk assessment prior to first flight of any spacecraft as well as the need to continue to develop/refine BLEs so that they more accurately reflect the shape and material density variations inherent to the actual debris environment.


*Keywords:* Orbital debris; Risk assessment; MMOD; Shape effects; Ballistic limit; CEV

## 1. Introduction

One of the primary mission risks tracked in the development of all spacecraft is that due to micro-meteoroids and orbital debris (MMOD). Micrometeoroids are naturally occurring objects that originate primarily from comets and asteroids. They orbit the sun and are present throughout the solar system. Orbital debris describes objects in Earth orbit due to human presence in space and originates primarily from spacecraft or launch vehicles. Orbital debris is concentrated at low Earth orbit (LEO; generally between 160 and 2000 km above the Earth's surface) with another peak at geosynchronous Earth orbit (GEO; 36,000 km above the Earth's surface).

Both types of particles, especially those larger than 0.1 mm in diameter, contain sufficient kinetic energy due to their combined mass and velocities to cause serious damage to crew members and spacecraft. MMOD may cause functional and/or structural damage to components like

* Corresponding author. Tel.: +1 573 341 4787; fax: +1 573 341 4729.
*E-mail address:* wschon@mst.edu (W.P. Schonberg).

0273-1177/$36.00 
doi:10.1016/j.asr.2010.11.007

pressure vessels, electronics, windows, etc., or may cause secondary effects by degrading systems (most notably the Thermal Protection System, or TPS) that fail during later mission phases (e.g., entry). In general, in LEO the risk from micrometeoroids is comparable to orbital debris (although orbital debris velocities tend to be lower than those of micrometeoroids, the relative flux of orbital debris in LEO is higher than that of micrometeoroids in LEO), beyond LEO the risk is predominately from micrometeoroids, and beyond GEO the risk is completely due to micrometeoroids.

The process used to assess MMOD risk consists of three elements: environment, damage prediction, and damage tolerance. The environment describes the particulate threat a spacecraft might encounter in terms that currently include velocity, directionality, and size during its mission. Damage prediction describes the extent of damage that will occur when an object, with specified physical characteristics, trajectory, and velocity, impacts a target, also of specified characteristics. Damage tolerance is a description of a failure criterion that is, how much damage can be withstood before unacceptable consequences occur in an impacted target. Failure criteria are often expressed in terms of an allowable depth of penetration into an impacted material, or whether or not penetration of a critical system occurs. Failure criteria are defined for each component that may be impacted by an MMOD particle and are used together with damage predictor equations in the development of the Ballistic Limit Equation, or BLE, for a particular component. As such, a BLE defines the critical diameter of an impactor necessary to reach a defined damage threshold such as perforation or maximum allowed penetration depth.

In the NASA Constellation Program (CxP), MMOD design requirements are set forth in terms of the probability that an impact event will cause Loss of Crew (LOC), Loss of Mission (LOM), and Loss of Crew or Vehicle (LOCV). LOC/LOM and LOCV values are specified for each of the three mission profiles defined for Orion: Crew Exploration Vehicle (CEV); Lunar Sortie/Lunar Outpost; and, International Space Station (ISS). All three profiles include launch from and return to the Earth's surface, the differences being the intermediate destinations and length of time for each mission. The Lunar Sortie mission includes a journey from the Earth to the Lunar surface, a nine day period of exploration on the Lunar surface, and then a return to Earth. The Lunar Outpost mission is to transfer personnel to permanent facilities on the Lunar surface, where they would stay for up to six months. The ISS mission is to rendezvous with the ISS and remain docked for a period of up to six months. Risk due to MMOD is rolled-up into the overall vehicle risk for each of the missions.

The Orion CEV is designed to carry up to six crew members on ISS missions and four for Lunar missions. The four major elements of the Orion spacecraft, the Spacecraft Adaptor (SA), the Service Module (SM), the Crew Module (CM), and the Launch Abort System (LAS) are shown in Fig. 1.

Of particular interest is the Orion CM since it serves as the habitable space for the crew. At the forward (top) end of the CM is the unpressurized compartment containing landing equipment (parachute systems), navigation equipment, and the docking mechanism. Below the forward compartment is the crew cabin. The crew cabin forms the habitable volume for human occupation. Along with the crew, their gear, and life support systems, the crew cabin carries avionics and electrical power distribution systems. Beneath the crew cabin is the base compartment. The base compartment is an unpressurized toroidal volume containing components of the reaction control subsystem, environmental control subsystem and landing subsystem.

The CM TPS (shown in Fig. 2) is designed to meet thermal protection requirements, but also serves as the MMOD protective barrier. The backshell TPS covers the crew cabin and the forward compartment. Each TPS tile is bonded to a Nomex® strain isolator pad (SIP), which is in turn

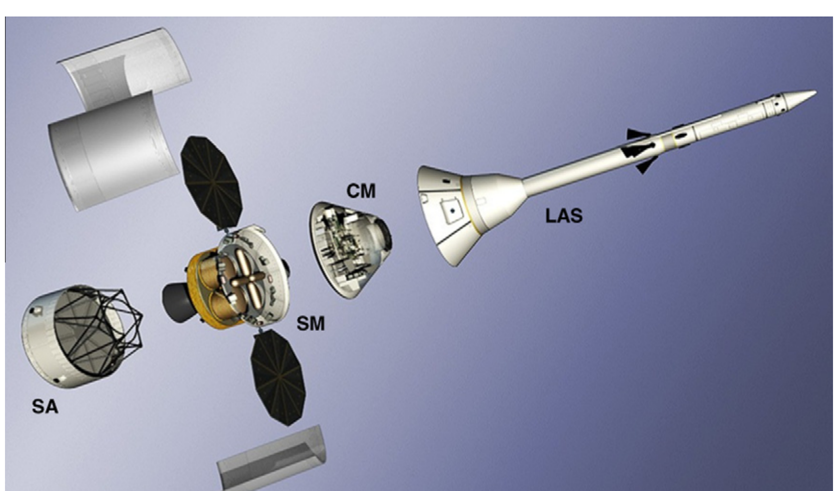


Fig. 1. Exploded view of the Orion spacecraft.

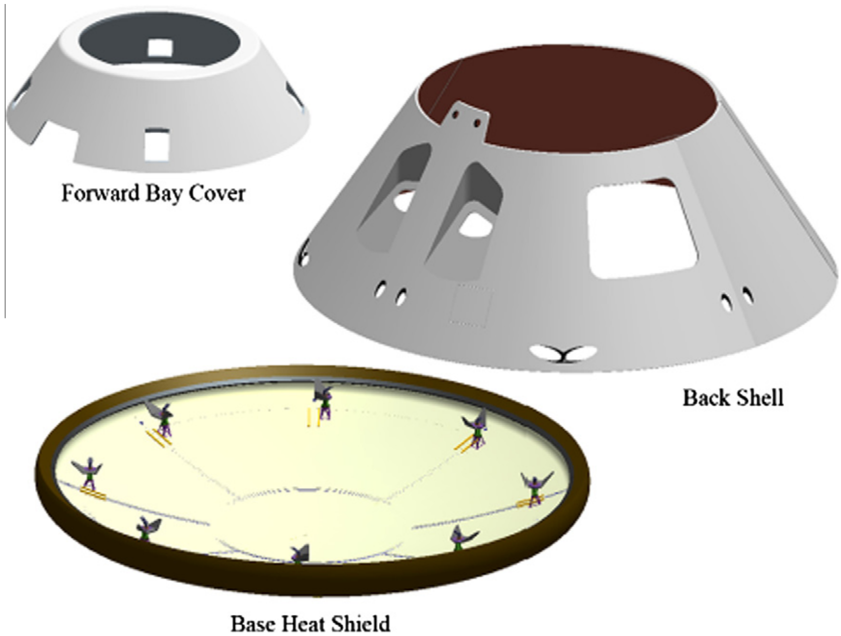


Fig. 2. Orion crew module TPS.

bonded to titanium honeycomb structure. The base heat shield is an ablative cover on the bottom (aft) of the crew module designed to dissipate the thermal load experienced during entry.

Orbital debris risk assessments for the Orion vehicle, as well as the Shuttle, Space Station and other satellites use BLEs that have been developed using high speed impact test data and results from numerical simulations that have used spherical projectiles. However, spheres are not expected to be a common shape for orbital debris. Rather, orbital debris fragments might be better represented by other regular or irregular solids. Historically, NASA's orbital debris models have been presented in terms of size rather than shape and mass because size is a parameter more directly linked to radar observables and hypervelocity testing. For these purposes, NASA defines "size" as a one-dimensional parameter, called *characteristic length*, computed as the average of the three, orthogonal, physical dimensions of the object: $L_C = \mathrm{CL} = (X + Y + Z)/3$, where the three lengths are specified as the longest dimension ($X$), the longest dimension perpendicular to the first ($Y$), and a third that completes the triad ($Z$). These measurements are illustrated in Fig. 3 using an image of a fragment from the SOCIT4 (SOCIT = Satellite Orbital-Debris Characterization Impact Test) ground-based impact experiment as described by Reynolds et al. (1998).

A major recommendation from a recent review of Bumper II, the software application used by NASA to perform MMOD risk analyses, called for the creation of shape and material parameters in future orbital debris environments, and to characterize the effect of these shapes on orbital debris damage predictions (NASA Engineering and Safety Center, 2005). In light of this recommendation, the objectives of the work presented in this paper are to:

- examine the general construction of NASA's current orbital debris (OD) model;
- explore the potential variations in orbital debris mass and shape that are possible when using particle characteristic length to define particle size (instead of assuming spherical particles); and,
- considering specifically the Orion vehicle, perform an orbital debris risk sensitivity study taking into account variations in particle mass and shape as noted above.

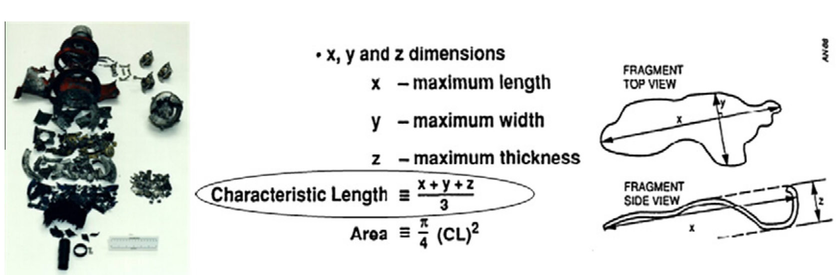


Fig. 3. Debris size as characteristic length.

The sensitivity study performed considered three scenarios to account for variations in mass and shape:

- Case 1: Reduced mass based on satellite and upper stage fragmentation models;
- Case 2: Reduced mass, non-spherical shapes, impact orientations; and,
- Case 3: BLEs reformulated strictly in terms of characteristic length, where both mass and non-spherical shape effects are considered together.

## 2. Orbital debris model sources

The orbital debris model currently used by NASA, ORDEM2000, is based on both empirical measurements of the environment and first-principles approaches to modeling the sizes of the debris particle (Liou et al., 2002). The resulting orbital debris environment is returned as OD particle flux (number of impacts/year/exposed spacecraft area) in terms of OD particle characteristic length ($L_C$). Fig. 4 summarizes the approaches used to determine OD flux in terms of regimes of OD particle $L_C$.

As can be seen in Fig. 4, above $L_C \sim 5$ mm, particle radar cross-section (RCS) measurements are converted to particle $L_C$ using a size estimation model (SEM) developed by Liou et al. (2002). The SEM is based on an analysis of 39 debris fragments in the 1–10 cm size range. These fragments were the product of two ground-based impact experiments, both involving an 85 g cylindrical aluminum projectile traveling at 5.5 km/s. In one test (shot 6470), the target consisted of two water-filled aluminum spheres covered by an open-ended cylindrical shroud (Krisko et al., 2000). In the other (shot 6472), the target was a scale model interceptor rocket (Johnson et al., 2001). The physical dimensions of each fragment were recorded, and laboratory experiments were conducted to characterize their radar signatures at several wavelengths. The product of the analysis was a relatively straightforward correlation function to convert from RCS to $L_C$ (Maclay et al., 1989).

Below $L_C \sim 1$ mm, orbital debris particles are estimated from crater and hole measurements in spacecraft surfaces returned from Earth orbit. Returned surfaces do provide a record of the number of impacts over a given time period and often some information on impact angle and impactor material type can be extracted. However, it can be difficult to explicitly and uniquely determine both the speed and size (or mass) of the impacting particle. That is, a surface crater or hole may have been created by a small, high-velocity projectile, but a larger, slower particle might have been responsible as well. Given some evidence that the crater or hole was created by an orbital debris particle (generally substantiated by examining the material remaining in the crater or on the edge of the hole), the process used by NASA to arrive at a solution in this regime assumes that the impacting particle was (1) a sphere, and (2) traveling at average orbital debris velocity (approx. 8.5 km/s). Once the size of the impacting debris particle has been determined, it is added to the orbital debris database and presented as a characteristic length.

For $L_C$ between 1 mm and 5 mm, particle sizes are interpolated from the neighboring particle populations of 100 μm and 1 cm. As shown in Fig. 3, observations down to approximately 3 mm from the Goldstone radar are used, however, to provide some corroboration. It is interesting to note that this interpolated region overlaps with the range of particle $L_C$ that is deemed most critical in terms of CEV failure.

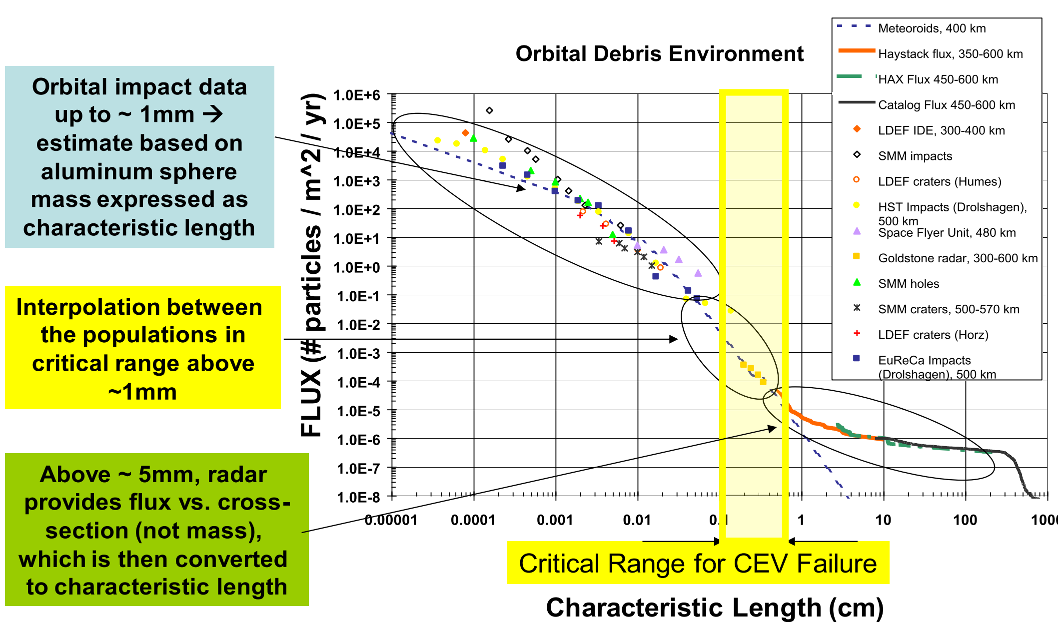


Fig. 4. Orbital debris model data sources.

## 3. Characterization of the orbital debris environment

The most basic hypervelocity ballistic limit or damage predictions use the kinetic energy or momentum of the impacting particle (relative to the target) to describe the damage inflicted to the target. Since mass and velocity are elements defining both of these quantities, their characterization is a prerequisite to performing hypervelocity penetration analyses, and subsequently risk analyses, of orbiting spacecraft. Other items, such as the obliquity of the particle relative to the spacecraft surface, as well as the shape and orientation of the particle, are also of interest.

A number of different ground-based experiments, including the SOCIT tests (which collected fragments from a series of impact tests that included an actual spacecraft) and European Space Operations Centre (ESOC) tests (which collected similar fragments from impact tests against a mockup of an upper stage), have generated mass distributions for typical orbital debris fragments that could be expected to impact spacecraft. These mass distributions can be plotted versus their measured characteristic length as shown in Figs. 5–8.

For the purposes of performing penetration risk analyses, NASA currently assumes that the shape of the impacting orbital debris particle is a sphere, with a diameter equal to the particle characteristic length. When plotted against the experimental fragment distributions shown in Figs. 5–8, it is apparent the masses of spheres with diameters equal to $L_C$ values above the "crossing points" are higher than the masses of the corresponding actual fragments at those characteristic lengths. As such, when $L_C$ exceeds the "crossing point" value, the kinetic energy associated with realistic (i.e. non-spherical) orbital debris fragments having those $L_C$ values is actually lower and less penetrating than currently assumed, an assumption which in turn currently leads to an over-prediction of risk. Virtually all of the particles in the fragment distributions shown in Figs. 5–8 have $L_C$ values above their respective "crossing point" values,

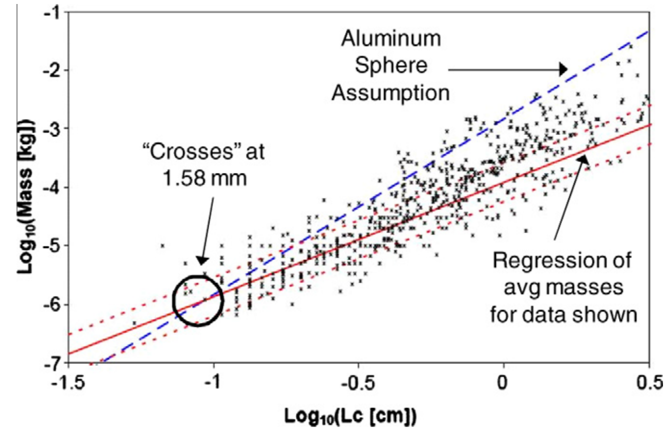


Fig. 6. Comparing mass of satellite fragments to aluminum spheres, revised SOCIT data (Matney, 2008).

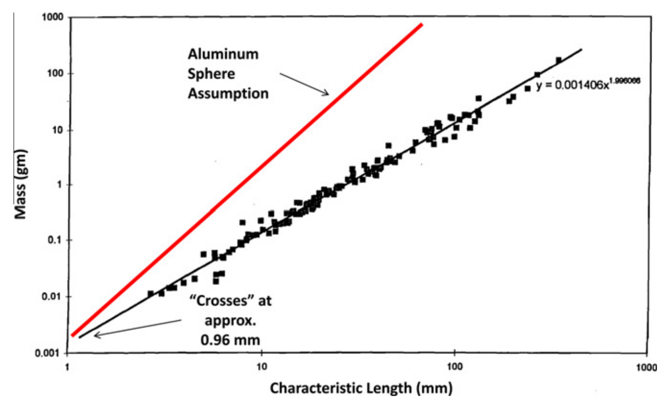


Fig. 7. Comparing mass of upper stage fragments to aluminum spheres, ESOC data (Fucke et al., 1993).

which indicates that virtually all of the particles are plate-like and hardly any are sphere-like (see also Krisko et al., 2008). Offsetting this to some degree, however, is the simplifying presumption of shape – the debris particles are taken to be spherical. For a given mass, it has been shown that many particle shapes are more penetrating than

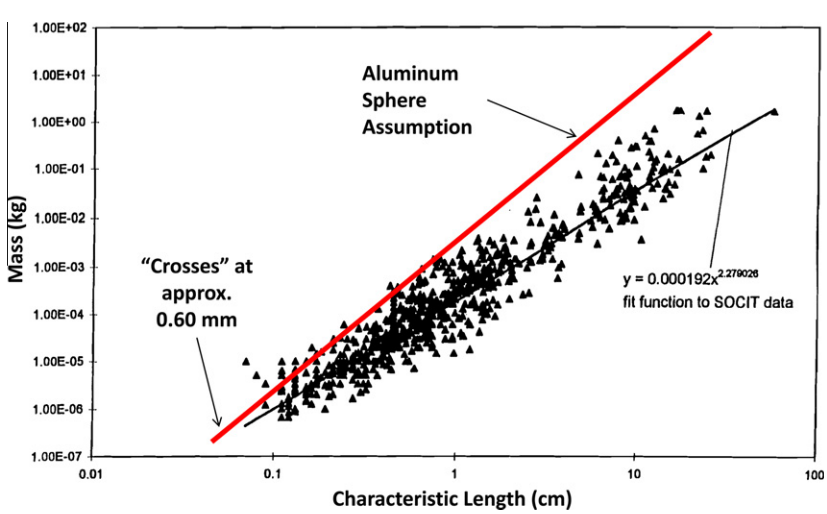


Fig. 5. Comparing mass of satellite fragments to aluminum spheres, original SOCIT data (Reynolds et al., 1998).

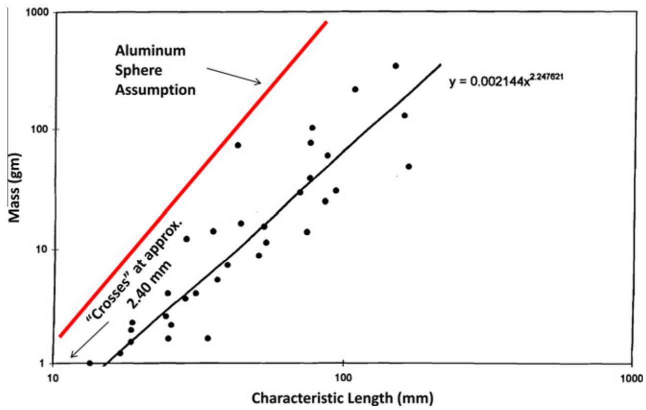


Fig. 8. Comparing mass of RCS fragments to aluminum spheres (Reynolds et al., 1998).

a sphere, stemming primarily from the less efficient particle disruption that occurs with shock waves propagating through irregular impactors.

An actual orbital debris fragment, therefore, will be either more or less penetrating than that being estimated by the solid sphere of the same size (characteristic length equal to spherical diameter), depending on which of these two effects dominates. The fragment will be less penetrating because of the smaller mass, but may be more penetrating because of the irregular shape. Three cases were developed to explore the effects on spacecraft failure of including mass and shape as part of an expanded orbital debris environment definition. The assumptions used and results obtained are discussed in the following sections.

## 4. Analysis case studies

### *4.1. Case 1: Effect of debris mass distribution on penetrating flux*

For the purposes of this analysis, the mass distributions for the ESOC experiment shown in Fig. 7 and for the SOCIT experiment shown in Fig. 5 were used to modify the orbital flux that is used by Bumper II, as shown in Fig. 9. In this approach, particle mass above a "crossing point" characteristic length (0.96 mm for the ESOC distribution, 1.58 mm for the selected SOCIT distribution) is taken from the appropriate fragment mass distribution regression line, that is, it corresponds to an aluminum sphere of a smaller diameter. Below a "crossing point" characteristic length, the mass value is taken to be that of an aluminum sphere having a diameter equal to the same characteristic length as in the original orbital debris flux.

The modified flux of aluminum spheres derived from each of the two mass distributions is shown in Fig. 10. It is interesting to note the ten-fold difference in flux at ~6 mm between current assumptions and a mass-based sphere approach for both distributions. For the Orion vehicle TPS, where the critical orbital debris size is much smaller (between 1 mm and 3 mm), the reduction of flux is lower. However, for systems such as the Orion SM, and for the ISS manned modules where the size of critical orbital debris penetrations is above 6 mm for many shield types, the preliminary assessment indicates a large potential decrease in assessed risk may be possible with such a consideration.

Table 1 summarizes the results of the orbital debris risk sensitivity analysis performed for the Orion vehicle backshell TPS, reflecting the majority of the assessed Orion vehicle MMOD risk (NASA Engineering and Safety Center, 2009). The MMOD risk analysis tool used was developed for previous US government program MMOD risk analyses and modified as needed for this study. The tool reads in files generated by the meteoroid or debris environment model and computes the total penetration risk on a specified group of surfaces. In terms of input/output functionality the method is analogous to Bumper II, but the detailed implementation is organized and coded differently.

For the Orion backshell TPS risk analysis, each panel was treated as a sector on the surface of a cone. A finite

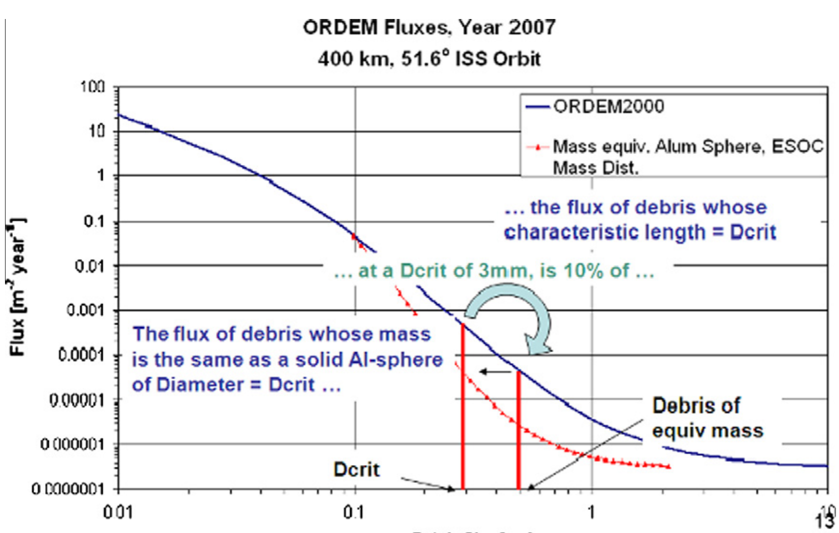


Fig. 9. Comparison of fluxes: ORDEM2000 and revision based on ESOC data.

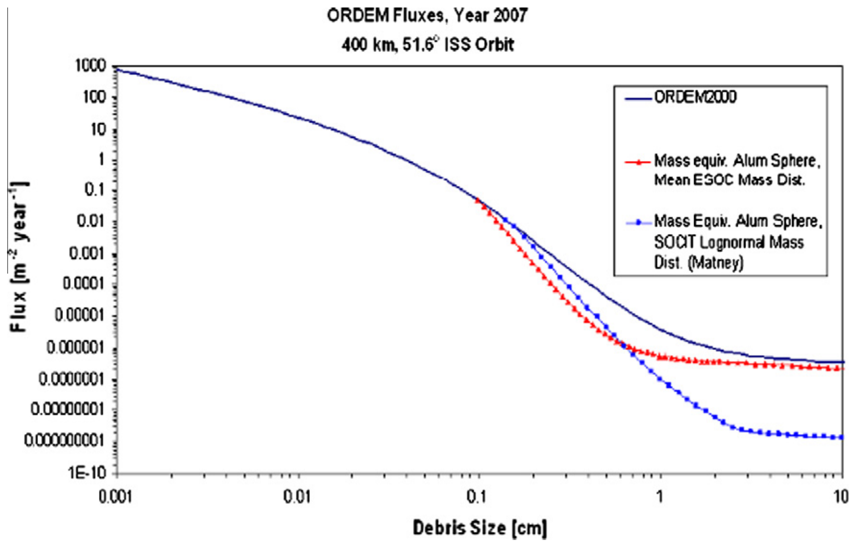


Fig. 10. Flux comparisons: ORDEM2000 and revision based on empirical mass distributions.

Table 1
Results of Case 1: effect of orbital debris distribution on LOC or LOCV risk.

| Mass distribution | Fraction of risk assessed using current OD model[a] |
|---|---|
| Mean ESOC | 0.25 |
| Matney/SOCIT | 0.74 |

[a] Backshell TPS only.

element model was developed in which each panel was divided into many flat surface elements. Each flat surface element was 1° wide and ran the entire length of the panel. The total flux was broken down into components defined by the particle impact velocity and direction. For each flat surface element, the code swept through all particle flux components. For cases that use velocity and orientation-dependent debris particle shape factors, the code also swept through particle orientations.

For each flux component and orientation, the BLE for the TPS was used to determine the critical particle diameter that resulted in penetration to the allowable depth. The BLE accounted for particle impact velocity and angle on the surface, as well as particle density; critical particle diameter was scaled by a shape factor if necessary (see subsequent discussion). The flux was then interpolated from the input flux versus size. If a flux versus mass curve was input, the scaled critical particle size was converted to critical mass assuming a spherical shape. The resulting flux was then weighted by the projected surface element area, which accounted for the Orion vehicle and panel orientation. The flux was also weighted by (1) the probability of impact velocity direction for that flux component, and (2) the probability of particle orientation to yield the probability of penetration of the surface element by that flux component. The penetration probabilities for all flux components, particle orientations, and surface elements were then summed and scaled by the mission duration to yield the total probability of penetration.

It is seen from results in Table 1 that, depending on the mass distribution used, more realistic mass representations of orbital debris appear to produce a predicted backshell TPS risk that is between 25% and 74% of current predictions that are obtained using aluminum spheres. However, there are a number of concerns with using either of these fragment mass distributions in their current form.

- At least two regressions have been performed of the SOCIT data: one presented in the NASA Standard Breakup Model (SBM) report and shown in Fig. 5 and another offered by NASA as shown in Fig. 6. It is possible that one or both of the data sets presented have missing data points.
- The SOCIT data at the lower sizes are binned, and masses and sizes are blended into the regressions using average and weighted values.
- The SOCIT data collection and analysis at the lower sizes is believed to have been measured by sifting it through screens, lending to uncertainty in the distribution. If so, they were not measured using the standard definition of characteristic length, and sizes may have been assigned simply by the size of the sifting screen holes.
- These data sets represent a small sample of ground tests with particular characteristics. SOCIT was intended to simulate a spacecraft fragmentation, using a real satellite. Most of the on-orbit fragmentations are rocket bodies, however, and those material distributions are likely different.

Despite these concerns, based on the results obtained thus far we believe that assessed spacecraft penetration risk would be reduced if a better mass distribution for orbital

debris fragments were to be developed and used in the construction of an improved orbital debris environment. However, as previously stated, the assessed risk is also dependent on the shape of the impacting particles. The next section will outline an attempt to determine the effect of particle shape on assessed risks.

### 4.2. Case 2: Effect of debris mass distribution and particle shape on penetrating flux

In considering the effect of orbital debris shape, we used a shape model from the NASA SBM report, originally designed to model the area-to-mass ratios of particles for re-entry considerations. In this SBM “flake” model, small debris (below a 1.66 mm characteristic length) are considered to be cubes, which become flakes (square plates) as the debris grows in size. The aspect ratio of the “flake” shape changes as it increases in size (becoming more “potato chip-shaped”) in order to better reflect the actual aspect ratio of orbital debris as measured in terms of RCS. As shown in Fig. 11, cubes and flakes more accurately represent debris shapes as collected from SOCIT ground-based satellite impact experiments than do spheres.

Although spheres present the same profile to a target regardless of their impact orientation, cubes and flakes vary considerably in this regard, resulting in different penetration effects depending on their specific orientation. As a result, the number of potential shape and orientation combinations that may be examined is literally unlimited. It is this characteristic that has likely prevented their inclusion in orbital debris risk assessments. To render this situation more manageable, an approach was used that selected a small number of fragment views that represented a wide variety of orientations while limiting the number of analysis runs considering particle orientation at impact.

Fig. 12 shows that a regular solid (e.g., flake, cube, or cylinder) may be considered in 26 views, with each view separated by 45° increments in the rotation axes from one another. Each arrow emanating from the cube in the upper left corner of Fig. 12 represents a potential velocity vector. For the SBM-based flake impacting a normal surface, symmetry reduces these 26 views to the five unique orientation cases listed in Fig. 12; for a cube, this results in the three unique cases shown. Assuming each of the 26 resulting views occurs with equal likelihood, the frequencies of each unique case (summing to 26 total views) can be derived as shown in Fig. 12.

In this study, shape and orientation effects at a given mass were determined for a typical TPS tile and a Whipple Shield. The primary tool used to model the TPS impacts is the Fast Aerial Target Encounter Penetration (FATEPEN) model, a set of fast-running algorithms that simulate the penetration of spaced target structures by fragments, long rods, and other regular projectiles (Yatteau et al., 2005). FATEPEN’s capability to examine the effect of non-spherical shapes into multi-plate aluminum targets renders it an important and immediately available tool for determining orbital debris penetration effects into typical spacecraft shielding materials. Whipple Shield impacts were modeled using the Autodyn software package.

Figs. 13 and 14 show that FATEPEN produces good correlation to NASA’s prediction for penetration of spheres into TPS throughout the orbital debris velocity range, for both normal and 45° obliquities, lending confidence to subsequent “flake” predictions. Once the suitability of using FATEPEN to model spherical particle impacts on TPS targets was established, the next step in the process

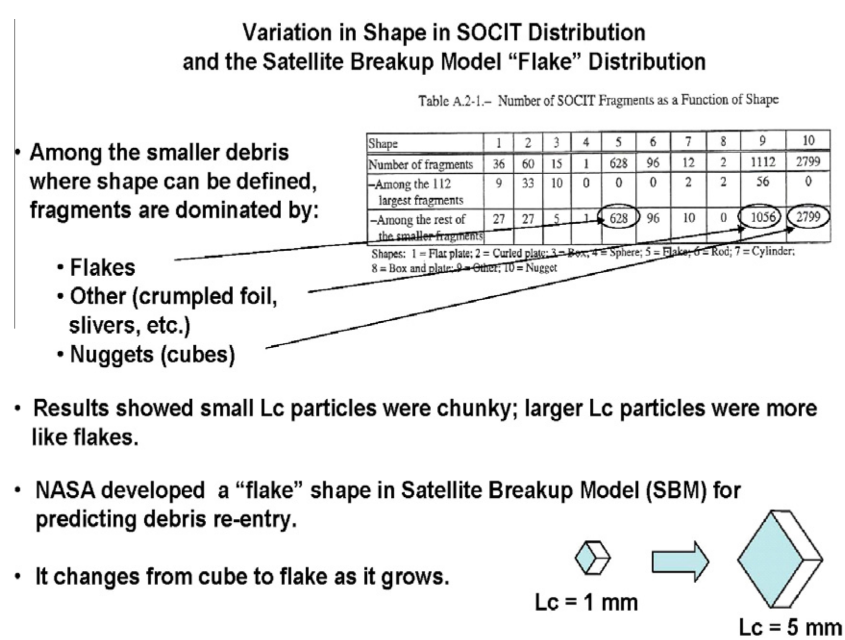


Fig. 11. Summary of fragment shapes resulting from SOCIT tests.

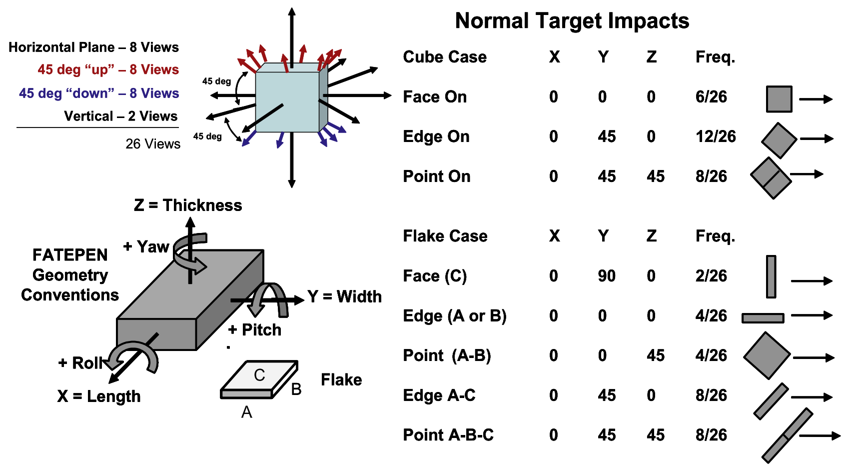


Fig. 12. Orientations considered in 26-view methodology.

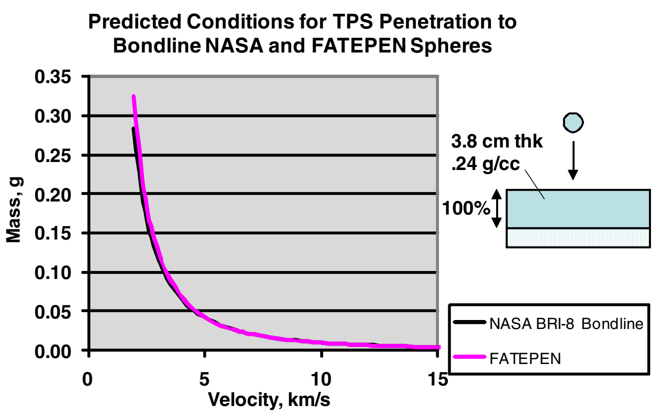


Fig. 13. Comparison of NASA to FATEPEN predictions for 100% TPS penetration, normal impact, spherical projectile.

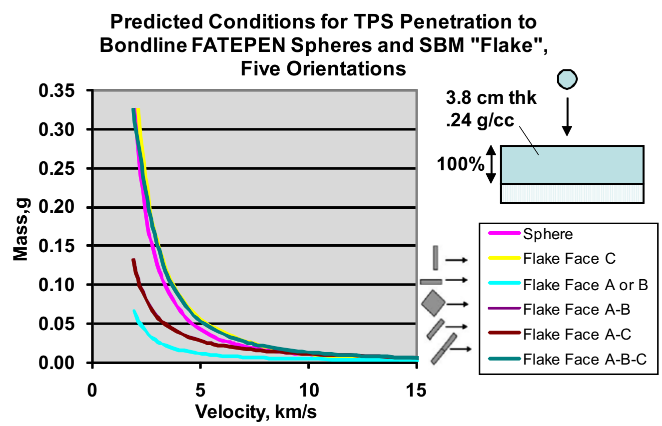


Fig. 15. Predicted TPS tile BLEs for a sphere and an SBM flake at various impact orientations, normal impact.

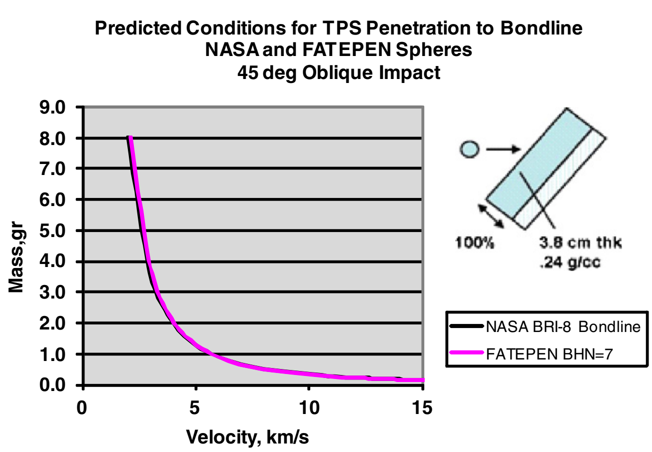


Fig. 14. Comparison of NASA to FATEPEN predictions for 100% TPS penetration, 45° impact, spherical projectile.

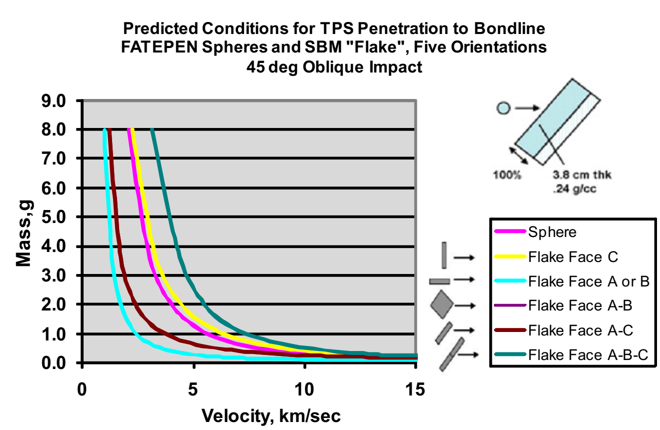


Fig. 16. Predicted TPS tile BLEs for a sphere and an SBM flake at various impact orientations, 45° impact.

was to develop mass-based ballistic limit equations/curves for the orientations noted above, shown in Figs. 15 and 16 for normal impact and 45° obliquity impact cases, respectively. These mass-based ballistic limit curves were then converted to equivalent diameter curves for spherical particles, and combined using the weights for the five orientations shown in Fig. 12 to produce a single effective or weighted average diameter-based BL curve (see Figs. 17

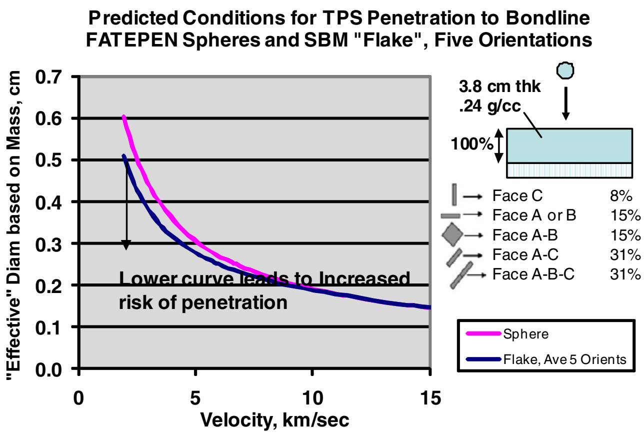


Fig. 17. Weighted average BLE for TPS targets, normal impact.

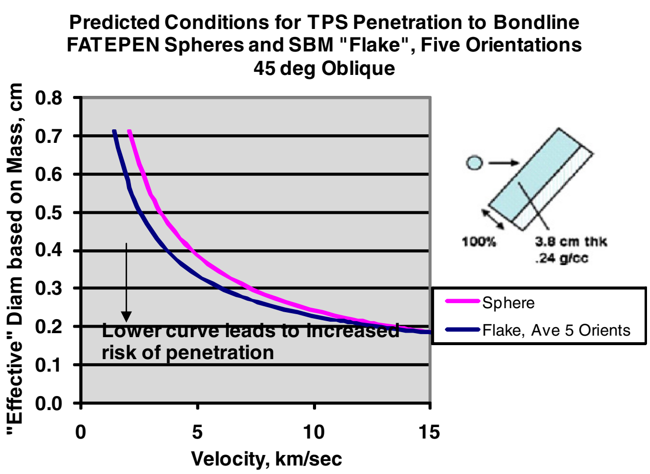


Fig. 18. Weighted average BLE for TPS targets, 45° impact.

and 18 for the weighted-average normal and 45° impact BL curves, respectively). For example, at 5 km/s (~0.06 g), the "Face C" ballistic limit mass in Fig. 15 would be converted to a sphere of 3.6 mm diameter, multiplied by a frequency of 2/26 (from Fig. 12), and then added to the results of such diameter-frequency calculations from the four other orientations in Fig. 15 to yield the weighted average diameter of 2.7 mm based on mass for that impact velocity (see Fig. 17).

Finally, these curves were used to create look-up tables of BL diameter multiplicative factors that could subsequently be applied to any TPS and Whipple Shield BL curves developed for aluminum spheres in order to take into account the impacts of non-spherical particles on such targets. A similar procedure was used to derive factors to determine effect of non-spherical impacts on Whipple Shields, although these factors were developed for normal impact (Williamsen et al., 2008); see Figs. 19 and 20. The application of these factors to a variety of Orion vehicle structures of different thicknesses, standoffs and obliquities might raise some concern regarding accuracy of this approach. However, given the preliminary nature of this study, it was hoped that the results obtained using this approach would yield a rough order estimate on effect of shape when applied to various mass distributions.

Table 2 summarizes the results of the Bumper II orbital debris risk sensitivity assessment performed by NASA for the entire Orion vehicle and the orbital debris risk analysis performed for the Orion vehicle backshell TPS. The MMOD risk assessment tool used to generate the results in Table 1 was used to generate the results in Table 2, but now also using the shape factors described above. Depending on the mass distribution used, the use of more realistic mass representations of orbital debris plus shape effects can produce either higher (1.20–1.24 for the SOCIT distribution) or lower risk (0.79–0.59 for the ESOC distribution) compared to aluminum spheres.

In retrospect, we believe that the "Case 2" methodology we used to examine the effect of including both mass and

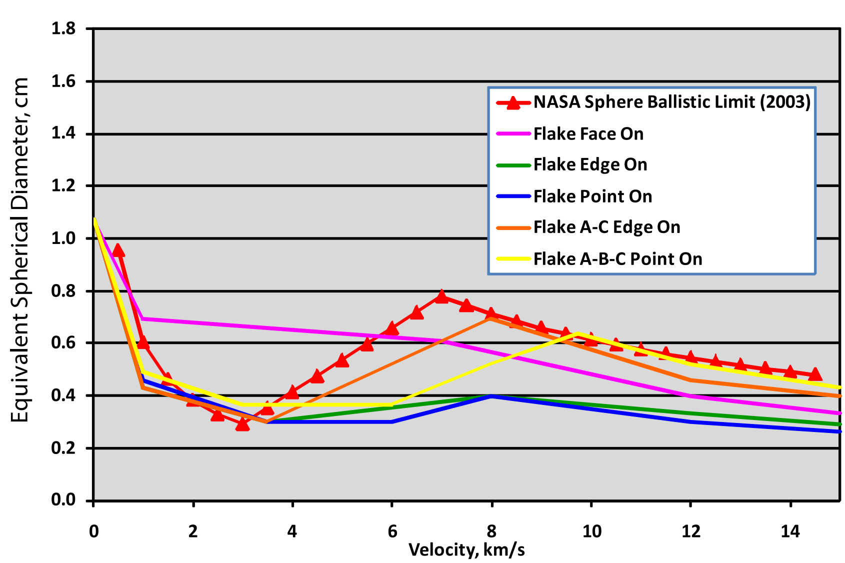


Fig. 19. Predicted Whipple Shield BLEs for a sphere and an SBM flake at various orientations, normal impact.

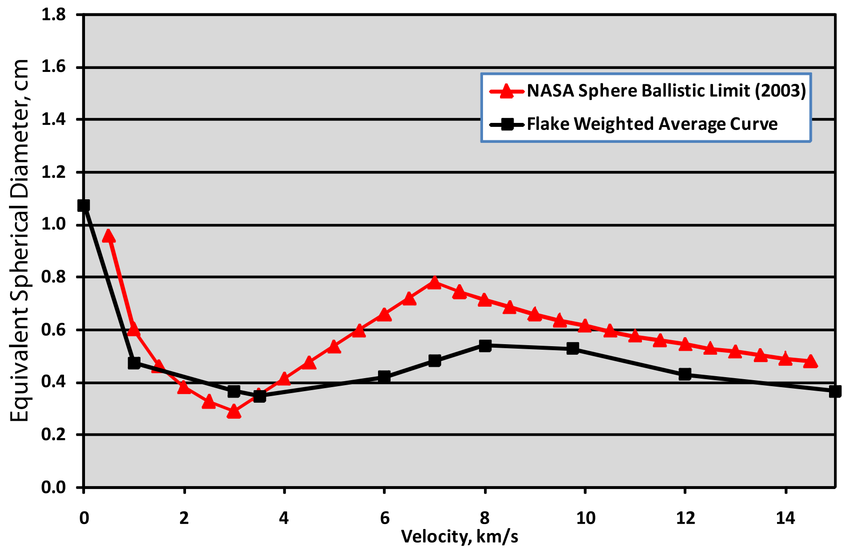


Fig. 20. Weighted average BLE for Whipple Shield targets, normal impact.

Table 2
Summary of results of Case 1 and Case 2 mass and shape sensitivity studies: effect of orbital debris distribution with particle shape effect on LOC or LOCV risk.

| Mass distribution | Source | Fraction of risk assessed using current OD model | |
|---|---|---|---|
| | | Mass distribution effect | Shape effect added to mass distribution effect |
| Mean ESOC | This study | 0.25[a] | 0.59[a] |
| | NASA (2009) | N/A | 0.79 |
| Matney/ SOCIT | This study | 0.74[a] | 1.24[a] |
| | NASA (2009) | N/A | 1.20 |

[a] Backshell TPS only.

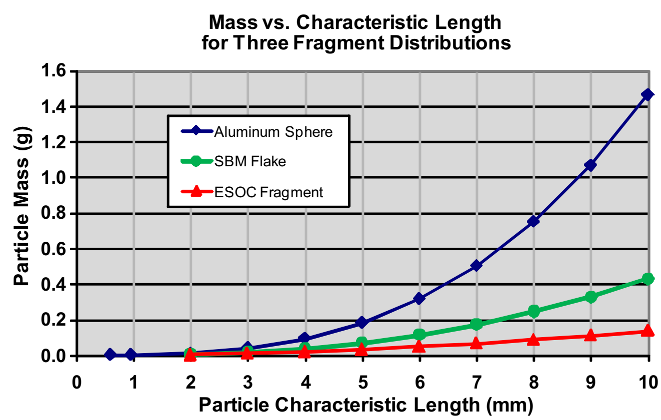


Fig. 21. Mass comparisons for sphere, SBM flake, and ESOC fragments having the same characteristic lengths.

shape considerations on spacecraft damage was flawed and produced overly conservative estimates (that is, over-predictions) of spacecraft risk. This methodology embodied a "two step" approach that applied a separately derived shape factor to a flux distribution that had already been adjusted for mass (recall Figs. 9 and 10). In doing this, it employed an immediate (not gradual) shape transition to a damaging SBM flake for orbital debris diameters above the mass transition point (0.95 mm for the ESOC distribution and 1.579 mm for the SOCIT distribution). On the other hand, the mass reduction factor sloped off gradually, not showing fuller effect until higher effective diameters were reached. This disjoint between mass and shape favored the more damaging effects of shape without considering equally the beneficial effects of mass reduction. Because of this deficiency, we developed another method to examine the combined effects of shape and mass on Orion vehicle orbital debris risk, which is discussed in the next section.

### 4.3. Case 3: BLEs reformulated strictly in terms of characteristic length

In this approach, the ballistic limit curves for TPS are derived directly in terms of characteristic length, applying results from FATEPEN to the shapes called out in the SBM flake model. Fig. 21 shows that fragments derived from the SBM flake model already account for reduced mass compared to a sphere, but are slightly higher than that of the experimental fragment distribution such as SOCIT. As such, ballistic limit curves incorporating this shape would reflect both the beneficial effects of reduced mass and the (somewhat conservative) effects of shape on spacecraft risk. An additional advantage of this approach (over the "two step" approach in Case 2) is the ability to apply the ballistic limit curve directly to the original ORDEM 2000 flux (recall Fig. 4), rather than apply them to a flux distribution that has been artificially adjusted for a separately derived mass distribution as in Figs. 9

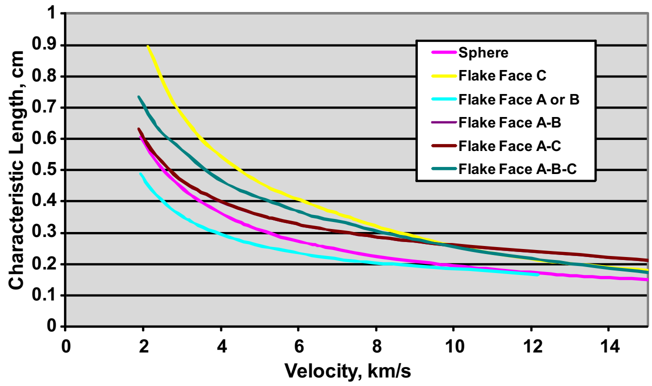


Fig. 22. Ballistic limit for TPS penetration (to bondline) for five SBM flake orientations, normal impact.

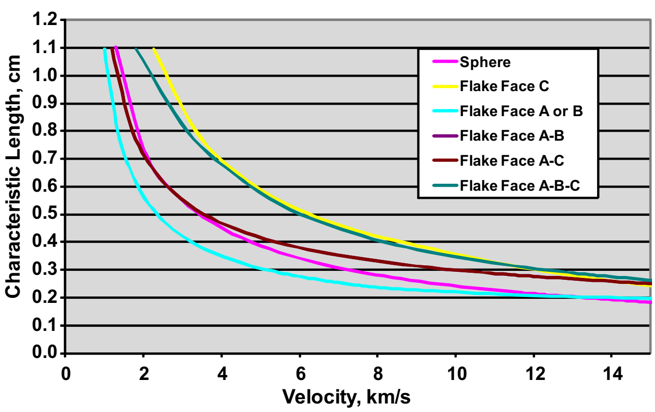


Fig. 23. Ballistic limit for TPS penetration (to bondline) for five SBM flake orientations, 45° obliquity impact.

and 10. In developing this approach, the following steps were taken:

- The masses and characteristic lengths for SBM flakes from 1 mm through 10 mm were calculated, with higher flake aspect ratios corresponding to larger characteristic lengths.
- FATEPEN was run to obtain the impact velocity (at both 0° and 45° angles) that penetrates to the bond line for the five different orientations.
- This information was then used to develop plots of penetrating velocity as a function of characteristic length.
- Using these plots, a table of penetrating characteristic length as a function of impact velocity was created, interpolating the penetrating characteristic lengths to find values at integer velocity values.
- Ratios of flake penetrating characteristic length to sphere penetrating characteristic length were determined for each impact orientation.
- These ratios were applied as growth or reduction factors to the computed TPS critical diameters for aluminum spheres.
- Original flux values for these characteristic lengths were then found and used to compute Orion vehicle risk.

The Case 3 procedure differs significantly from that used in Case 2 in the following regards:

- In Case 3, there is no "averaging" of five different orientations into a single value for characteristic length as in Case 2, which was used (alone) for determining risk of penetration. An average particle produced by a linear weighted average does not produce the same risk as five different particles taken individually, because the relationship of probability to each particle size is highly nonlinear.
- By using a ballistic limit curve based on characteristic length that is developed directly for each of the five orientations, the Case 3 procedure avoids the disjoint in Case 2 of using an immediate (not gradual) shape transition for orbital debris diameters above the mass transition point, yet employing a mass reduction factor that slopes off gradually and does not show its full effect until higher effective diameters are reached.

Table 3
Sphere-to-SBM flake adjustment factors for TPS tile targets, normal impact.

| Velocity (km/s) | Characteristic length | | | | | | $L_C$ ratios to sphere | | | | |
|---|---|---|---|---|---|---|---|---|---|---|---|
| | Sphere | C | A or B | A–B | A–C | A–B–C | C | A or B | A–B | A–C | A–B–C |
| 2 | 0.594 | 0.900 | 0.474 | 0.613 | 0.613 | 0.780 | 1.515 | 0.798 | 1.032 | 1.032 | 1.313 |
| 3 | 0.442 | 0.676 | 0.353 | 0.465 | 0.465 | 0.564 | 1.529 | 0.799 | 1.052 | 1.052 | 1.276 |
| 4 | 0.362 | 0.545 | 0.294 | 0.399 | 0.399 | 0.464 | 1.506 | 0.812 | 1.102 | 1.102 | 1.282 |
| 5 | 0.308 | 0.461 | 0.260 | 0.356 | 0.356 | 0.412 | 1.497 | 0.844 | 1.156 | 1.156 | 1.338 |
| 6 | 0.271 | 0.407 | 0.234 | 0.325 | 0.325 | 0.367 | 1.502 | 0.863 | 1.199 | 1.199 | 1.354 |
| 7 | 0.245 | 0.362 | 0.215 | 0.303 | 0.303 | 0.338 | 1.478 | 0.878 | 1.237 | 1.237 | 1.380 |
| 8 | 0.223 | 0.322 | 0.203 | 0.286 | 0.286 | 0.306 | 1.444 | 0.910 | 1.283 | 1.283 | 1.372 |
| 9 | 0.207 | 0.287 | 0.194 | 0.271 | 0.271 | 0.279 | 1.386 | 0.937 | 1.309 | 1.309 | 1.348 |
| 10 | 0.193 | 0.258 | 0.185 | 0.258 | 0.258 | 0.255 | 1.337 | 0.959 | 1.337 | 1.337 | 1.321 |
| 11 | 0.181 | 0.236 | 0.177 | 0.249 | 0.249 | 0.236 | 1.304 | 0.978 | 1.376 | 1.376 | 1.304 |
| 12 | 0.171 | 0.216 | 0.168 | 0.239 | 0.239 | 0.218 | 1.263 | 0.982 | 1.398 | 1.398 | 1.275 |
| 13 | 0.162 | 0.202 | 0.160 | 0.230 | 0.230 | 0.202 | 1.247 | 0.988 | 1.420 | 1.420 | 1.247 |
| 14 | 0.155 | 0.190 | 0.154 | 0.220 | 0.220 | 0.188 | 1.226 | 0.994 | 1.419 | 1.419 | 1.213 |
| 15 | 0.150 | 0.178 | 0.150 | 0.210 | 0.210 | 0.174 | 1.187 | 1.000 | 1.400 | 1.400 | 1.160 |

Table 4
Sphere-to-SBM flake adjustment factors for TPS tile targets, 45° impact.

| Velocity (km/s) | Characteristic length | | | | | | $L_C$ ratios to sphere | | | | |
|---|---|---|---|---|---|---|---|---|---|---|---|
| | Sphere | C | A or B | A–B | A–C | A–B–C | C | A or B | A–B | A–C | A–B–C |
| 2 | 0.744 | 1.120 | 0.562 | 0.708 | 0.708 | 1.050 | 1.505 | 0.755 | 0.952 | 0.952 | 1.411 |
| 3 | 0.550 | 0.889 | 0.421 | 0.554 | 0.554 | 0.821 | 1.616 | 0.765 | 1.007 | 1.007 | 1.493 |
| 4 | 0.450 | 0.694 | 0.350 | 0.469 | 0.469 | 0.680 | 1.542 | 0.778 | 1.042 | 1.042 | 1.511 |
| 5 | 0.386 | 0.586 | 0.306 | 0.416 | 0.416 | 0.577 | 1.518 | 0.793 | 1.078 | 1.078 | 1.495 |
| 6 | 0.342 | 0.510 | 0.276 | 0.380 | 0.380 | 0.503 | 1.491 | 0.807 | 1.111 | 1.111 | 1.471 |
| 7 | 0.306 | 0.460 | 0.254 | 0.352 | 0.352 | 0.448 | 1.503 | 0.830 | 1.150 | 1.150 | 1.464 |
| 8 | 0.279 | 0.418 | 0.240 | 0.331 | 0.331 | 0.406 | 1.498 | 0.860 | 1.186 | 1.186 | 1.455 |
| 9 | 0.259 | 0.386 | 0.228 | 0.313 | 0.313 | 0.373 | 1.490 | 0.880 | 1.208 | 1.208 | 1.440 |
| 10 | 0.241 | 0.356 | 0.220 | 0.299 | 0.299 | 0.346 | 1.477 | 0.913 | 1.241 | 1.241 | 1.436 |
| 11 | 0.226 | 0.326 | 0.214 | 0.287 | 0.287 | 0.324 | 1.442 | 0.947 | 1.270 | 1.270 | 1.434 |
| 12 | 0.213 | 0.300 | 0.208 | 0.276 | 0.276 | 0.305 | 1.408 | 0.977 | 1.296 | 1.296 | 1.432 |
| 13 | 0.202 | 0.278 | 0.204 | 0.267 | 0.267 | 0.289 | 1.376 | 1.010 | 1.322 | 1.322 | 1.431 |
| 14 | 0.192 | 0.258 | 0.200 | 0.258 | 0.258 | 0.275 | 1.344 | 1.042 | 1.344 | 1.344 | 1.432 |
| 15 | 0.183 | 0.241 | 0.197 | 0.251 | 0.251 | 0.262 | 1.317 | 1.077 | 1.372 | 1.372 | 1.432 |

Figs. 22 and 23 show a set of FATEPEN derived ballistic limit curves for five SBM flake orientations against the same TPS shield as used in Case 1, considering both normal and 45° impact obliquities. Of course, one of the problems with any ballistic limit derivation technique for a complex shape is the limited number of obliquities used in employing the factors. However, as shown in Tables 3 and 4, the adjustment factors for ballistic limits compared to spheres of the same characteristic lengths were not appreciably different for the 0° and 45° impact obliquities, lending confidence to their applicability to a variety of possible impact obliquities, especially between 0° and 45°.

Using these adjustment factors in the MMOD risk analysis for the Orion backshell TPS, the debris risk level was found to be approximately 54% of the risk currently assumed using aluminum sphere assumptions. This assessment uses characteristic length as does the orbital debris environment model, matches the mass-to-area ratio of orbital debris particles in the 1 mm–1 cm range, and approximates the mass distribution versus characteristic length for orbital debris particles obtained from ground based experiments. We note that we believe these results to be still somewhat conservative, that is, they may still over-predict spacecraft risk, for the following reasons:

- The SBM flake is constructed of points and flat surfaces that tend to be more penetrating than the more rounded "nuggets" derived from SOCIT experiments.
- The results are dictated by one (of the five) impact orientations – the addition of more orientations may well lower these risk estimates.

## 5. Conclusions

While the results of the work performed for this study are preliminary, they do show that continuing to use aluminum spheres in spacecraft risk assessments could result in an *over*-design of its MMOD protection systems. In such a case, the spacecraft could be heavier than needed, could cost more than needed, and could cost more to put into orbit than needed. The results obtained in this study also show the need to incorporate effects of mass and shape in mission risk assessment prior to first flight of any spacecraft as well as the need to continue to develop/refine BLEs so that they more accurately reflect the shape and material density variations inherent to the actual debris environment. This can be accomplished by performing hypervelocity impact tests with a variety of projectile materials and shapes, using validated hydrocode models to obtain adjustment factors for existing BLEs, developing BLEs for materials/densities in forthcoming debris environment models that allow risk assessment processes to take advantage of model environment refinements, and developing BLEs for non-spherical projectiles to decrease uncertainties. The result of such activities would be spacecraft design and risk assessment processes that include more appropriate models of spacecraft response when threatened by the orbital debris environment.

## Acknowledgement

The authors would like to acknowledge the support provided by the NASA Engineering and Safety Center that made this work possible.

## References

Fucke, W., Sdunnus, H., Klinkrad, H. Population Model of Small Size Space Debris. Final Report, ESOC Contract No. 9266/90/D/MD, Noordwijk, The Netherlands, 1993.

Johnson, N.L., Krisko, P.H., Liou, J.C., Anz-Meador, P.D. NASA's new breakup model of EVOLVE 4.0. Adv. Space Res. 28 (9), 1377–1384, 2001.

Krisko, P.H., Horstman, M., Fudge, M.L. SOCIT4 collisional break-up test data analysis with shape and materials characterization. Adv. Space Res. 41, 1138–1146, 2008.

Krisko, P.H., Reynolds, R.C., Bade, A., Eichler, P., Jackson, A.A., Matney, M.J., Siebold, K.H., Soto, A., Opiela, J.N., Hall, D.T., Liou, J.C., Anz-Meador, P.D., Kessler, D.J. EVOLVE 4.0 User's Guide and Handbook. LMSMSS-33020, Houston, Texas, 2000.

Liou, J.C., Matney, M.J., Anz-Meador, P.D., Kessler, D.J., Jansen, M., Theall, J.R. The New NASA Orbital Debris Engineering Model ORDEM2000. NASA/TP 2002-210780, Houston, Texas, 2002.

Maclay, T.D., Hinga, M., Madler, R. Analysis of Shot 6470 Fragments. Internal Interim Research Report # SD-89-02T, CCAR, University of Colorado, Boulder, Colorado, 1989.

Matney, M.J. A Simple Analysis of the Effects of Mass Distributions on Penetrating Flux. NASA Johnson Space Center, E-mail Correspondence with NESC, Houston, Texas, October 3, 2008.

NASA Engineering and Safety Center. BUMPER II Micrometeoroid and Orbital Debris Independent Technical Assessment. Report No. RP-05-66, Washington, DC, 2005.

NASA Engineering and Safety Center. Independent Review of Constellation (Cx) Orion Vehicle Micro-meteoroids and Orbital Debris (MMOD) Risk Analysis. Report No. NESC-RP-08-00468, Washington, DC, 2009.

Reynolds, R.C., Bade, A., Eichler, P., Jackson, A.A., Krisko, P.H., Matney, M.J., Kessler, D.J., Anz-Meador, P.D. NASA Standard Breakup Model, 1998 Revision. Lockheed Martin Space and Mission Systems and Services, Report No. LMSMMSS-32532, Houston, TX, 1998.

Williamsen, J., Schonberg, W.P., Evans, H., Evans, S. A comparison of NASA, DoD, and hydrocode ballistic limit predictions for spherical and non-spherical shapes versus dual- and single-wall targets, and their effects on orbital debris penetration risk. Int. J. Impact Eng. 35, 1870–1877, 2008.

Yatteau, J., Zernow, R., Recht, G., Edquist, K. FATEPEN (Version 3.0.0) Terminal Ballistic Penetration Model: Volume I – Analyst's Manual. Applied Research Associates, Naval Surface Weapons Center, Dahlgren, Virginia, 2005.